Reducing Impurities in Medical Images Based on Curvelet Domain

Vo Thi Hong Tuyet(✉) and Nguyen Thanh Binh

Faculty of Computer Science and Engineering,
Ho Chi Minh City University of Technology, Ho Chi Minh City, Vietnam
vothihongtuyet.dhbk@gmail.com, ntbinh@cse.hcmut.edu.vn

Abstract. Medical image quality greatly affects the diagnostic process. Most of the tasks of increasing the quality of medical images are deblurring or denoising process. These tasks are the difficult problems in medical image processing because they must keep edge features. In the cases, the medical images that have blur combined with noise are a more difficult problem. In this paper, we proposed a method for reducing impurities in medical images based on curvelet domain. The proposed method uses curvelet coefficient combined with augmented lagrangian function to denoising combined with deblurring in medical images. For evaluating the results of the proposed method, we have compared the results with the other recent methods available in literature.

Keywords: Deblurring · Denoising · Curvelet transform · Augmented lagrangian method · Medical image.

1 Introduction

In medical fields, image becomes a useful tool for specialists. For medical images, there are many types of medical images such as plain X-ray, computed tomography (CT), nuclear medicine imaging, ultrasound, magnetic resonance imaging (MRI), etc. Most of medical images have blur, noise or pair because of many reasons such as [4] machine specification, surroundings, etc. Noise in images always makes the undesirable appearance, but the noise can cover and reduce or lose the visibility of certain features within the image. Increasing the quality of medical images becomes difficult problem for image processing.

In the past, many methods are proposed to improve the quality of images: wavelet transform [1], discrete wavelet transform (DWT) [2, 3], … Although DWT is a powerful tool signal and image analysis but it has three serious disadvantages [4]: shift sensitivity, poor directionality and lack of phase information. Several methods have provided solutions for decreasing these disadvantaged such as: contourlet transform [5], nonsubsampled contourlet transform [6, 7], ridgelet transform [8, 9], curvelet transform [10, 11], etc. The results were significantly improved when using the above methods for denosing or deblurring.

The curvelet transform, a new X-let transform multiscale transforms, is like the wavelet transform, but it has directional parameters, and contains elements with a

P.C. Vinh et al. (Eds.): ICTCC 2014, LNICST 144, pp. 306–319, 2015
DOI: 10.1007/978-3-319-15392-6_29

very high degree of directional specificity. The results of curvelet transform for denoising are good. In case that the medical images have noise combined with blur, the results of the above methods in some cases are not good.

Stanley [12] proposed augmented lagrangian method for deblurring or denoising. This method has given the good results, special for deblurring or denoising, but in case of blur and noise pair, this is a difficult problem. To handle this problem, deblurring process with blur and noise pair is applied.

In this paper, we proposed a method for reducing impurities in medical images based on curvelet domain. The proposed method uses curvelet coefficient combined with augmented lagrangian function to denoising combined with deblurring in medical images. For evaluating the results of the proposed method, we have compared the results with the other recent methods available in literature such as DWT [2], curvelet transform [10] and augmented lagrangian [12]. For performance measure, we have used Peak Signal to Noise ratio (PSNR) and Mean Square Error (MSE) and it has shown that the present method yields far better results.

The rest of the paper is organized as follows: in section 2, we described the basic of curvelet transform and augmented lagrangian functions; details of the proposed method are given in section 3; the results of the proposed method are presented in section 4 and our conclusions in section 5.

2 Background

2.1 Curvelet Transform

As the above mentioned, DWT has three serious disadvantages [4]: shift sensitivity, poor directionality and lack of phase information. The curvelet transform has provided solutions for decreasing these disadvantages.

Curvelets [10] are better than wavelet based transform in case of representing edges and other singularities along curves. Curvelets can be translated and dilated, similar to wavelet transform. At first decomposing the image into subbands, a curvelet's curve is displayed with width $\approx$ length^2. After decomposing, each scale is analyzed by a local ridgelet transform.

Similar to ridgelets, curvelets occur at all scales, locations, and orientations. However, while ridgelets have global length and variable widths, curvelets in addition to a variable width have a variable length and so does a variable anisotropy.

In wavelet transform, dyadic subbands are $[2^s, 2^{s+1}]$. But with discrete curvelet transform, the subbands have the nonstandard form $[2^{2s}, 2^{2s+2}]$. The basic process of the digital realization for curvelet transform is given as follows [10, 11]:

(i) Subband Decomposition. The image f is decomposed into subbands

$$f \mapsto (P_0 f, \Delta_1 f, \Delta_2 f, \ldots)$$

(ii) Smooth Partitionning. Each subband is smoothly windowed into "squares" of an appropriate scale (of sidelength ~2-s)

$$\Delta_s f \mapsto (w_Q \Delta_s f)_{Q \in Q_S}$$

where w_Q is a collection of smooth window localized around dyadic squares:

$$Q = [k_1 / 2^s, (k_1 + 1) / 2^s] \times [k_2 / 2^s, (k_2 + 1) / 2^s]$$

(iii) Renormalization. Each resulting square is renormalized to unit scale

$$g_Q = (T_Q)^{-1}(w_Q \Delta_S f), \qquad Q \in Q_S$$

(iv) Ridgelet Analysis. Each square is analyzed via the discrete ridgelet transform.

In this definition, the two dyadic subbands $[2^{2s}, 2^{2s+1}]$ and $[2^{2s+1}, 2^{2s+2}]$ are merged before applying the ridgelet transform.

2.2 Augmented Lagrangian Method

Stanley[12] proposed a algorithm which minimizes a total variation optimization problem for spatial-temporal data. This algorithm uses an augmented lagrangian method to solve the constrained problem. A linear shift invariant imaging system is modeled as [12]: $g = Hf + \eta$, where f $\in \mathbb{R}^{MN\times 1}$ is a vector denoting the unknown (potentially sharp) image of size M x N, g $\in \mathbb{R}^{MN\times 1}$ is a vector denoting the observed image, $\eta \in \mathbb{R}^{MN\times 1}$ is a vector denoting the noise, and the matrix H $\in \mathbb{R}^{MN\times MN}$ is a linear transformation representing convolution operation.

And the goal of image restoration is from the observed image g, algorithms will recover f. Two problems are considered as:

$\underset{f}{\text{minimize}} \ \frac{\mu}{2}\|Hf - g\|^2 + \|f\|_{TV}$, which is known as the TV/L2 minimization

and

$\underset{f}{\text{minimize}} \ \mu\|Hf - g\|_1 + \|f\|_{TV}$, which is known as the TV/L1 minimization.

With equations, μ is a regularization parameter. The idea of the augmented lagrangian method is to find a saddle point and the alternating direction method (ADM) can be used.

3 The Proposed Method

Medical images, which have blur combined with noise, are very difficult to increase the quality of medical image process. In this section, we propose a new approach for image deblurring, with blur combined with noise pair that based on curvelet Transform combined with augmented lagrangian method.

In the proposed method, we divide image processing with blur combined with noise pair into two processes: denoising and deblurring. The proposed method includes two processes. The proposed method can be summarized as follows:

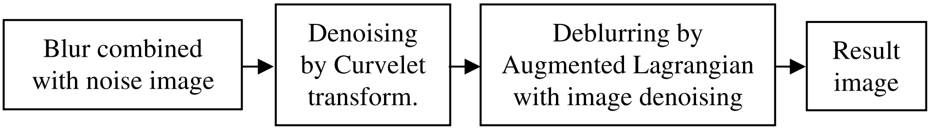

Fig. 1. The process of proposed method

Firstly, medical image denoising. The medical input images are the blur combined with noise images, we use curvelet transform for denoising the image, curvelet's process is as follows [10]:

1) apply the à trous algorithm with scales and set $b_1=b_{min}$
2) for $j=1, \ldots, j$ do
   a. partition the subband w_j with a block size b_j and apply the digital ridgelet transform to each block;
   b. if j modulo 2 = 1 then $b_{j+1}=2b_j$;
   c. else $b_{j+1}=b_j$

The sidelength of the localizing windows is doubled at every other dyadic subband. After this step, the input images had become image denoising.

Secondly, medical image deblurring. The blur combined with noise images have removed noise in curvelet domain in the above steps. However, the blur in images are not removed more. To remove the blur, we use augmented lagrangian for the output images, which output from the previous steps.

In here, we use augmented lagrangian TV/L2 algorithm [12] to remove the blur. The problem that we solve in TV/L2 minimization is $\underset{f}{\min imize}\ \frac{\mu}{2}\|Hf - g\|^2 + \|f\|_{TV}$

The idea of augmented lagrangian [12] is to find a saddle point of L(f, u, y); then, they use the alternating direction method (ADM) to solve f-subproblem and u-subproblem, with f-subproble and u-subproblem are considered as [12]:

$$f_{k+1} = \arg\min_{f} \frac{\mu}{2}\|Hf - g\|^2 - y_k^T(u_k - Df) + \frac{\rho_r}{2}\|u_k - Df\|^2$$

$$u_{k+1} = \arg\min_{u} \|u\|_1 - y_k^T(u - Df_{k+1}) + \frac{\rho_r}{2}\|u - Df_{k+1}\|^2$$

where ρ_r is a regularization parameter, y is the Lagrange multiplier, u = Df. Algorithm of TV/L2 can be summarized as follows [12]:

(i) Input: vector denoting the observed image and convolution matrix.
(ii) Input: regularization parameter, the isotropic total variation.
(iii) Set parameter with value default for $\rho_r = 2$.
(iv) Compute the matrices of the first-order forward finite difference operators along the horizontal, vertical and temporal directions.
(v) With not coverge do:
   - Solve the f-subproblem.
   - Solve the u-subproblem.

- Update the Lagrange multiplier.
- Update ρ_r.
- Check convergence, if false is continue.

4 Experiments and Results

In this section, we apply the procedure described in section 3 and achieving superior performance in our deblurring experiments as demonstrated in this section. For performance evaluation, we compare the results of the proposed method based on the curvelet transform combined with Augmented Lagrangian (CT-AL) with the other methods such as Discrete Wavelet Transform (DWT), Curvelet Transform (CT) and Augmented Lagrangian method (AL).

We test the above methods in a medical image dataset. This dataset includes different images of the sizes: 256 x 256, 512 x 512. The types of blurs are used Gaussian and Motion combined with Gaussian or Speckle noises which were added to these medical images. Hard thresholding is applied to the coefficients after decomposition in curvelet domain. All of the above methods are done on the same images at similar scale.

The quality of images is inproved by comparison with the value of Mean Square Error (MSE) and Peak Signal-to-Noise Ratio (PSNR). The MSE is defined as:

$$\text{MSE}=\sqrt{\frac{1}{\text{NxN}}\sum_{i=1}^{N}\sum_{j=1}^{N}(x_{i,j}-y_{i,j})^2}$$

where x is the image which has blur and noise; y is the image result and N x N is the size of the image. The PSNR is used as the measure of the quality of the reconstruction of the image deblurring or denoising, defined as:

$$\text{PSNR}=20\log_{10}\left(\frac{\text{MAX}_1}{\text{MSE}}\right)$$

where MAX_1 is the maximum pixel value of the image. The proposed method compared with DWT, CT, and AL method by the MSE and PSNR values. The smaller the value of MSE is, the better it is. The higher the value of PSNR is, the better it is. The images dataset includes more than 1000 medical images. In here, we show some test cases.

Figure 2 shows the deblurring of blur combined with noise image by Gaussian blur and Gaussian noise with our proposed method. Figure 3 shows the deblurring of blur combined with noise image by Gaussian blur and Speckle noise with our proposed method.

From Figure 2 and Figure 3 we see that the result of the proposed method is better than the other methods. Figure 4 and Figure 5 show the plot of PSNR, MSE values of different image deblurring methods corrupted with Gaussian blur combined with Gaussian noise.

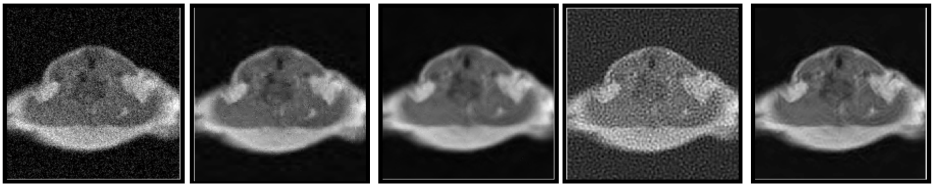

(a) (b) (c) (d) (e)

Fig. 2. Blur and noise image with Gaussian blur with Gaussian noise and deblurred images by different methods.
(a) Blur and noise image (PSNR = 21.6304 db). (b) Deblurred image by DWT (PSNR = 28.7178 db). (c) Deblurred image by CT (PSNR = 29.5102 db). (d) Deblurred image by AL (PSNR = 21.8365 db). (e) Deblurred image by CT-AL (PSNR = 30.1838 db).

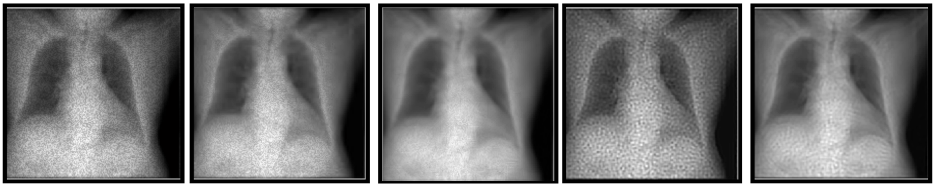

(a) (b) (c) (d) (e)

Fig. 3. Blur and noise image with Gaussian blur with Speckle noise and deblurred images by different methods.
(a) Blur and noise image (PSNR = 23.3928 db). (b) Deblurred image by DWT (PSNR = 24.8552 db). (c) Deblurred image by CT (PSNR = 25.6510 db). (d) Deblurred image by AL (PSNR = 23.9808 db). (e) Deblurred image by CT-AL (PSNR = 26.1718 db).

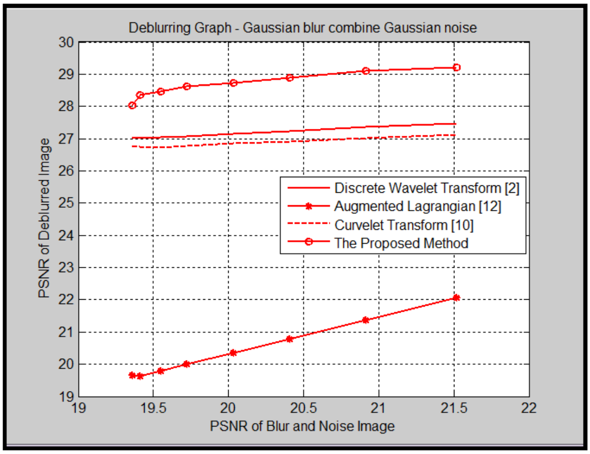

Fig. 4. Plot of PSNR values of deblurred images corrupted with Gaussian blur combined with Gaussian noise using different methods

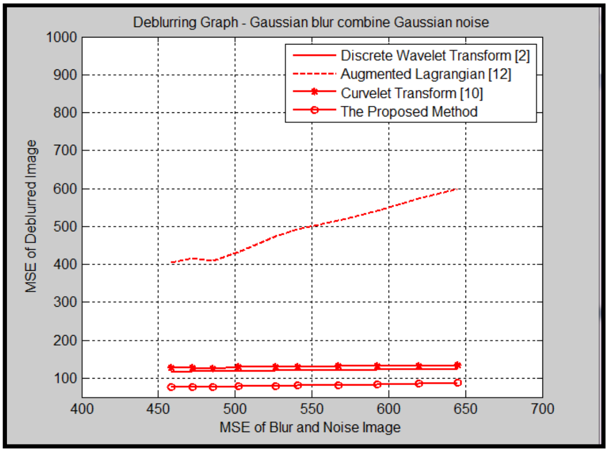

Fig. 5. Plot of MSE values of deblurred images corrupted with Gaussian blur and Gaussian noise using different methods

Figure 6 and Figure 7 show the plot of PSNR, MSE values of different image deblurring methods corrupted with Gaussian blur combined with Speckle noise.

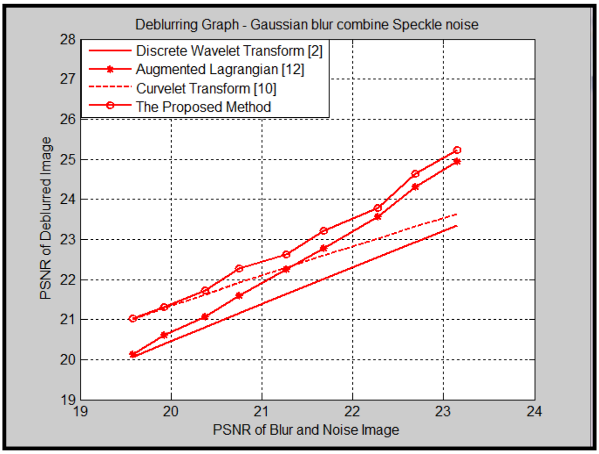

Fig. 6. Plot of PSNR values of deblurred images corrupted with Gaussian blur combined with Speckle noise using different methods

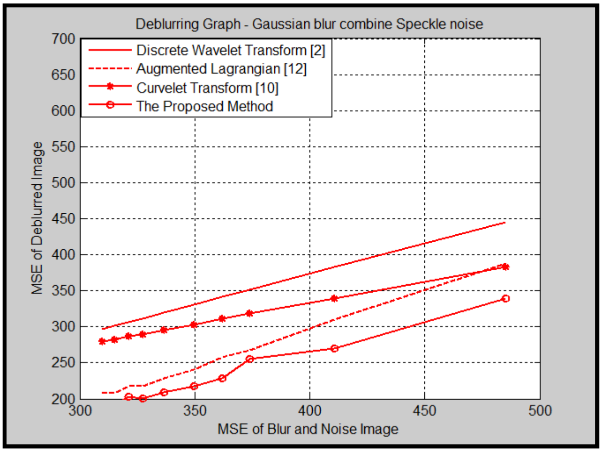

Fig. 7. Plot of MSE values of deblurred images corrupted with Gaussian blur combined with Speckle noise using different methods

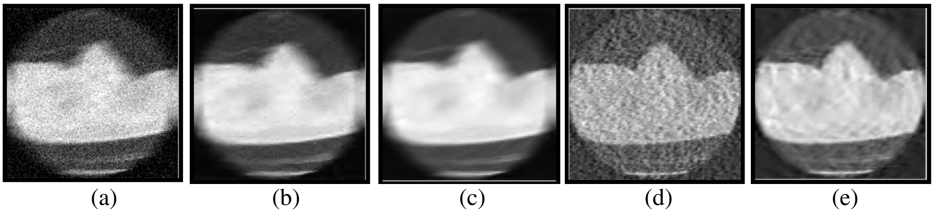

Fig. 8. Blur and noise image with Motion blur corrupted with Gaussian noise and deblurred images by different methods.

(a) Blur and noise image (PSNR = 17.7757 db). (b) Deblurred image by DWT (PSNR = 20.0554 db). (c) Deblurred image by CT (PSNR = 20.2554 db). (d) Deblurred image by AL (PSNR = 16.9942 db). (e) Deblurred image by CT-AL (PSNR = 20.5285db).

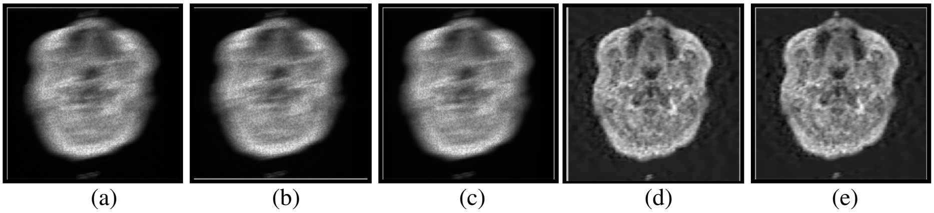

Fig. 9. Blur and noise image with Motion blur corrupted with Speckle noise and deblurred images by different methods.

(a) Blur and noise image (PSNR = 19.8879 db). (b) Deblurred image by DWT (PSNR = 19.8937 db). (c) Deblurred image by CT (PSNR = 19.9248 db). (d) Deblurred image by AL (PSNR = 24.3089 db). (e) Deblurred image by CT-AL (PSNR = 24.7597 db).

Figure 8 shows the deblurring of blur combined with noise image by Motion blur and Gaussian noise with our proposed method. Figure 9 shows the deblurring of blur and noise image by Motion blur and Speckle noise with our proposed method.

From Figure 8 and Figure 9 we see that the result of the proposed method is better than the other methods. Figure 10 and Figure 11 show the plot of PSNR, MSE values of different image deblurring methods corrupted with Motion blur and Gaussian noise.

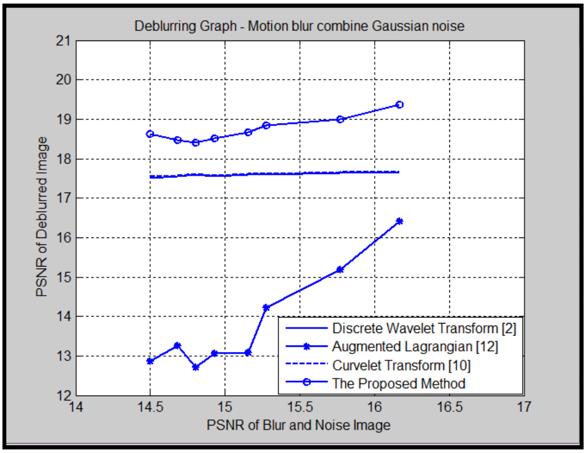

Fig. 10. Plot of PSNR values of deblurred images corrupted with Motion blur combined with Gaussian noise using different methods

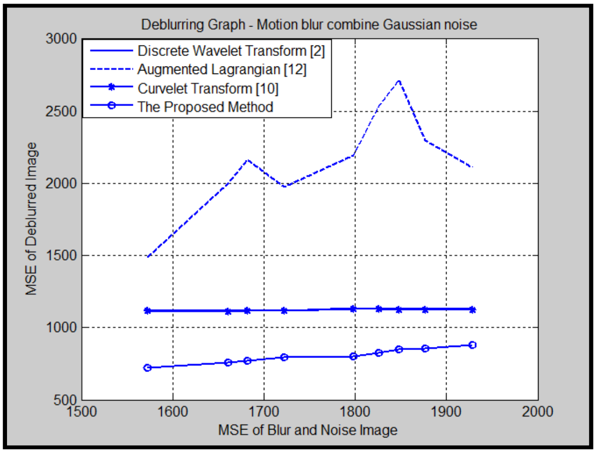

Fig. 11. Plot of MSE values of deblurred images corrupted with Motion blur combined with Gaussian noise using different methods

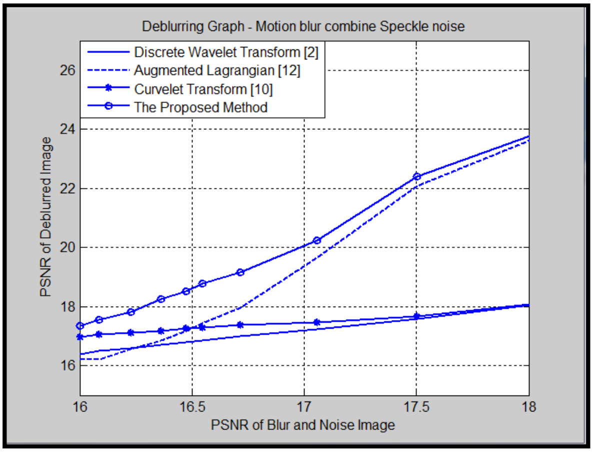

Fig. 12. Plot of PSNR values of deblurred images corrupted with Motion blur combined with Speckle noise using different methods

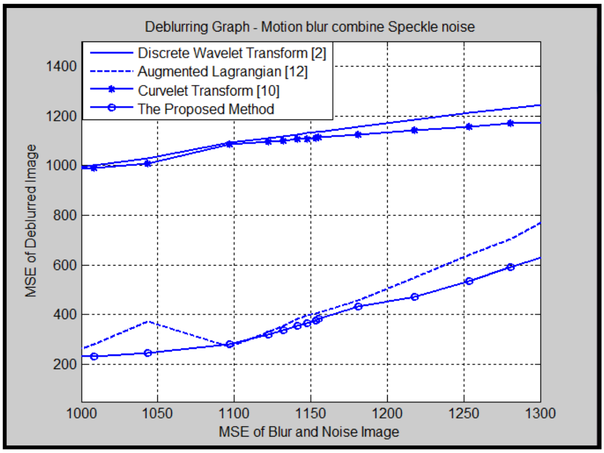

Fig. 13. Plot of MSE values of deblurred images corrupted with Motion blur combined with Speckle noise using different methods

Figure 12 and Figure 13 show the plot of PSNR, MSE values of different image deblurring methods corrupted with Motion blur and Speckle noise.

In the above figures, it is well observed that the proposed method performs better than Discrete Wavelet Transform, Curvelet Transform and Augmented Lagrangian method. We show some results in appendix.

5 Conclusions

In this paper, we propose deblurring for medical images in case that image has blur combined with noise. The proposed method is to divide into two processes: denoising and deblurring. In here, we use curvelet transform for denoising process; then, we apply augmented lagrangian method to remove blur into the result of image denoising. We test this proposed method in medical images. The results are very good in pairs: Gaussian blur combined with Gaussian noise, Gaussian blur combined with Speckle noise, Motion blur combined with Gaussian noise, Motion blur combined with Speckle noise.

From the results of the above section, we conclude that the proposed method works well and better than the other recent methods available in literature. With these results, we think the division of deblurring image pairs into two steps, and the attempt to improve the quality in every step will give the good results.

Appendix

Table A1. PSNR values (dB) of different denoised images using the image sizes with Gaussian blur combined with Gaussian noise

Test Image	Image Size	Blur & Noisy Image	DWT[2]	Augmented Lagrangian [12]	Curvelet Transform [10]	Proposed Method
1	256 x 256	22.9244	25.8099	23.7983	25.5685	**26.5559**
2		22.2133	24.2929	22.9969	24.3754	**25.3269**
3		21.0976	24.8965	21.6440	25.2272	**26.1492**
4		19.4362	23.7983	19.9117	23.9008	**25.0569**
5		18.2394	25.1596	18.1658	25.1750	**25.6090**
6		16.9048	20.9809	17.3390	20.7117	**21.6296**
7		17.5342	23.6197	17.7768	23.5211	**24.5133**
8		17.0701	23.7615	17.2127	23.5877	**24.3908**
9		19.9343	27.0370	20.0527	28.4109	**28.8235**
10		20.0474	26.0461	20.2580	26.2711	**27.2532**
11	512 x 512	29.1889	34.1455	30.3814	33.7877	**35.4287**
12		24.5894	25.868	26.4690	25.5396	**27.5126**
13		23.1588	24.3679	25.1043	24.0030	**26.1835**
14		26.6912	32.1044	27.6333	31.6351	**33.7255**
15		26.2812	32.2987	27.0246	31.8528	**33.6101**
16		22.9881	24.8190	24.7584	24.4512	**26.7523**
17		22.8137	24.9043	24.3170	24.5046	**26.5185**
18		24.0391	28.3583	25.1259	27.9272	**30.4065**
19		23.5482	29.3542	24.1043	29.0079	**30.3145**
20		20.5393	29.0540	20.6704	29.2314	**30.0370**

Table A2. PSNR values (dB) of different denoised images using the image sizes with Gaussian blur combined with Speckle noise

Test Image	Image Size	Blur & Noisy Image	DWT [2]	Augmented Lagrangian [12]	Curvelet Transform [10]	Proposed Method
1	256 x 256	25.3317	26.2724	26.9356	25.9678	**27.3101**
2		23.6729	23.8157	24.7394	24.5437	**25.4935**
3		26.5841	26.5859	28.6510	26.5935	**28.7674**
4		23.0049	23.2379	23.9696	24.0989	**25.1103**
5		22.3268	24.3122	22.7326	25.5115	**25.8778**
6		19.1728	20.1243	19.9501	20.9859	**21.8423**
7		21.7705	22.4099	22.7529	24.5911	**25.5676**
8		20.7059	21.9209	21.3406	24.7097	**25.5628**
9		25.5202	25.6334	25.7726	25.8730	**25.9703**
10		27.7495	28.0029	30.0571	28.6791	**31.0672**
11	512 x 512	27.5376	28.2788	27.8823	29.6975	**29.9848**
12		23.3779	24.9436	24.6555	25.3136	**26.8313**
13		22.6507	22.8481	24.2205	23.1493	**24.5772**
14		27.0762	27.5978	27.5625	28.5009	**28.7954**
15		31.1310	31.4597	33.0762	32.0104	**34.0305**
16		24.0044	24.1745	26.1215	24.3156	**26.4488**
17		24.0804	24.2322	26.0170	24.4191	**26.2889**
18		26.3336	26.7466	27.9941	27.0914	**28.7282**
19		26.8237	27.1567	27.5356	27.8142	**28.5943**
20		25.7610	26.0674	26.0722	26.9874	**27.2278**

Table A3. PSNR values (dB) of different denoised images using the image sizes with Motion blur combined with Gaussian noise

Test Image	Image Size	Blur & Noisy Image	DWT [2]	Augmented Lagrangian [12]	Curvelet Transform [10]	Proposed Method
1	256 x 256	20.6283	24.5833	18.3993	24.5046	**25.1109**
2		19.6985	21.8751	18.4899	22.0335	**23.2947**
3		16.6634	20.1343	14.3206	20.7545	**21.3162**
4		18.7020	21.3746	17.4078	21.4380	**23.5657**
5		20.0156	24.5744	17.3834	24.5559	**25.2453**
6		17.3715	18.8926	17.0862	18.8816	**20.5954**
7		18.3267	19.8430	18.1566	19.8492	**22.7888**
8		19.1747	20.6569	19.8055	20.6399	**23.7520**
9		23.7832	27.1146	22.1617	27.1975	**29.1118**
10		22.7712	24.2517	23.3973	24.2842	**27.2143**
11	512 x 512	24.3067	28.8253	22.3026	28.7308	**31.1969**
12		20.0452	21.5405	20.5063	21.5046	**24.4124**
13		18.2509	19.2933	19.7132	19.2843	**22.7128**
14		21.8895	25.3906	20.4410	25.3813	**28.6708**
15		22.0630	26.7441	19.8375	26.7041	**29.1133**
16		17.9709	19.4733	18.5724	19.4318	**23.0173**
17		17.9843	19.5816	18.2576	19.5591	**22.7241**

Table A3. *continued*

18		19.7384	22.9871	18.1821	22.9640	**25.9907**
19		20.4899	24.5673	18.4405	24.5432	**26.5373**
20		21.0241	26.4155	18.2516	26.4521	**28.0329**

Table A4. PSNR values (dB) of different denoised images using the image sizes with Motion blur combined with Speckle noise

Test Image	Image Size	Blur & Noisy Image	DWT [2]	Augmented Lagrangian [12]	Curvelet Transform [10]	Proposed Method
1	256 x 256	23.2239	23.9372	24.6089	23.9313	**25.5673**
2		21.0064	21.0957	22.2576	21.5293	**23.1924**
3		21.7457	21.8367	23.0025	22.2514	**24.1839**
4		19.2673	19.4222	20.8222	19.9200	**22.0299**
5		17.8965	20.0387	16.1796	20.9946	**21.9860**
6		13.1633	15.0743	10.8040	16.0336	**16.5820**
7		12.5757	14.4820	10.8717	16.3005	**17.3208**
8		16.0558	16.5649	18.7345	16.8521	**21.2138**
9		24.7997	24.8311	27.6666	24.9057	**28.0803**
10		20.5104	21.0270	20.3254	22.1575	**23.3486**
11	512 x 512	25.3272	25.6067	26.4289	26.0485	**28.0667**
12		19.5076	19.8676	22.7892	19.9695	**24.0304**
13		17.6062	17.6547	22.0296	17.7410	**22.2915**
14		23.1467	23.2775	25.7503	23.4773	**26.6989**
15		23.8223	24.1072	24.8569	24.6375	**26.1031**
16		17.5181	17.5862	22.1037	17.6776	**22.5206**
17		17.7036	17.7615	22.0898	17.8653	**22.4803**
18		21.1085	21.2521	24.0262	21.3906	**24.7144**
19		22.2176	22.3451	24.3521	22.5821	**25.2422**
20		23.0288	23.2136	22.5770	23.7427	**23.7650**

References

1. Strang, G.: Wavelets and dilation equations: A brief introduction. SIAM Review **31**(4) (1989)
2. Edwards, T.: Discrete Wavelet Transforms: Theory and Implementation (1992)
3. Kociolek, M., Materka, A., Strzelecki, M., Szczypínski, P.: Discrete Wavelet transform – derived features for digital image texture analysis. In: Proc. of International Conference on Signals and Electronic Systems, pp. 163–168 (2001)
4. Binh, N.T., Khare, A.: Image Denoising, Deblurring and Object Tracking, A new Generation wavelet based approach. LAP LAMBERT Academic Publishing (2013)
5. Do, M.N., Vetterli, M.: The contourlet transform: an efficient directional multiresolution image representation. IEEE Trans. Img. Processing, 2091–2106 (2005)
6. da Cunha, A.L., Zhou, J., Do, M.N.: Nonsubsampled Contourlet Transform: Theory, Design, and Applications. IEEE Trans. Img. Proc, 3089–3101 (2005)
7. da Cunha, A.L., Zhou, J., Do, M.N.: Nonsubsampled Contourlet Transform: Filter design and applications in denoising (2006)

8. Candes, E.J.: Ridgelets: Theory and Applications. Stanford University (1998)
9. Zhang, B.J., Fadili, M., Starck, J.L.: Wavelets, ridgelets and curvelets for poisson noise removal. IEEE Transactions on Image Processing, 1093–1108 (2008)
10. Starck, J.L., Candès, E.J., Donoho D.L.: The curvelet transform for image denoising. IEEE Trans. Image Processing, 670–684 (2002)
11. Binh, N.T., Khare, A.: Multilevel threshold based image denoising in curvelet domain. Journal of Computer Science and Technology, 632–640 (2010)
12. Chan, S.H., Khoshabeh, R., Gibson, K.B., Gill, P.E., Nguyen, T.Q.: An Augmented Lagrangian Method for Total Variation Video Restoration. IEEE Trans. Image Process. **20**(11), 3097–3111 (2011)
13. Khare, A., Tiwary, U.S.: A new method for deblurring and denoising of medical images using complex wavelet transform. IEEE (2005)
14. Ruikar, S.D., Doye, D.D.: Wavelet Based Image Denoising Technique. International Journal of Advanced Computer Science and Applications **2**(3) (2011)
15. Candes, E.J., Demanet, L., Donoho, D.L., Ying, L.: Fast Discrete Curvelet Transforms. Multiscale Modeling and Simulation **5**, 861–899 (2006)
16. Lina, J.M., Mayrand, M.: Complex Daubechies Wavelets. Journal of Applied and Computational Harmonic Analysis **2**, 219–229 (1995)